Exploring the Phototoxicity of Hypoxic Active Iridium(III)-Based Sensitizers in 3D Tumor Spheroids

Robin Bevernaegie,[†] Bastien Doix,[‡] Estelle Bastien,[‡] Aurélie Diman,[⊥,§] Anabelle Decottignies,[⊥] Olivier Feron,*[,‡] and Benjamin Elias*[,†]

[†]Institut de la Matière Condensée et des Nanosciences, Molecular Chemistry, Materials and Catalysis, UCLouvain, Place Louis Pasteur 1 Box L4.01.02, B-1348 Louvain-la-Neuve, Belgium

[‡]Institut de Recherche Expérimentale et Clinique, Pole of Pharmacology and Therapeutics, UCLouvain, Avenue Hippocrate 57 Box B1.57.04, B-1200 Woluwé-Saint-Lambert, Belgium

[⊥]Institut de Duve, UCLouvain, Avenue Hippocrate 75 Box B1.75.02, B-1200 Woluwé-Saint-Lambert, Belgium

S *Supporting Information*

ABSTRACT: Among all molecules developed for anticancer therapies, photodynamic therapeutic agents have a unique profile. Their maximal activity is specifically triggered in tumors by light, and toxicity of even systemically delivered drug is prevented in nonilluminated parts of the body. Photosensitizers exert their therapeutic effect by producing reactive oxygen species via a light-activated reaction with molecular oxygen. Consequently, the lowering of pO_2 deep in solid tumors limits their treatment and makes essential the design of oxygen-independent sensitizers. In this perspective, we have recently developed Ir(III)-based molecules able to oxidize biomolecules by type I processes under oxygen-free conditions. We examine here their phototoxicity in relevant biological models. We show that drugs, which are mitochondria-accumulated, induce upon light irradiation a dramatic decrease of the cell viability, even under low oxygen conditions. Finally, assays on 3D tumor spheroids highlight the importance of the light-activation step and the oxygen consumption rate on the drug activity.
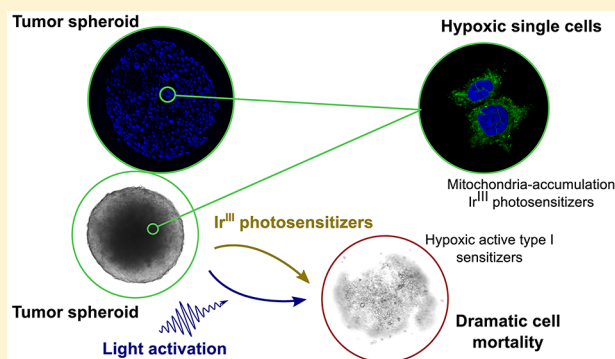
INTRODUCTION

Over the last decades, photodynamic therapy (PDT) has emerged as a promising method to treat diseases in diverse areas of medicine, especially in oncology.[1,2] Its features, including low systemic toxicity and minimally invasive procedure, make it an interesting alternative to conventional cancer therapies such as chemotherapy, radiotherapy, and surgery.[3] The photodynamic effect arises from a light-activated reaction between a photosensitizer (PS) and molecular oxygen.[1−3] The mechanisms are complex but can be divided into two main pathways, both inducing the production of reactive oxygen species (ROS) (Figure 1).[4] On one hand, type I processes involve a photoinduced electron transfer with biological substrates, leading after several steps to radical species such as superoxide ($O_2^{•−}$), hydroxyl ($OH^•$), and hydroperoxyl ($HO_2^•$). On the other hand, type II photoreactivity consists in the production of singlet oxygen ($^1O_2$) by a direct energy transfer.

For decades, research in cancer PDT has focused on the design of efficient photosensitizers to produce more $^1O_2$, which is the main mediator causing tissue damage.[4,5] Different generations of light-activatable molecules with an increased quantum yield of $^1O_2$ photoproduction (Φ_Δ) have been developed.[6,7] Efforts have been also made to improve light
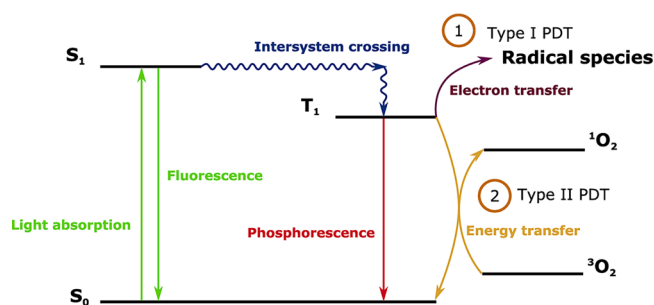

Figure 1. Simplified Jablonski diagram for classical production of ROS by a photosensitizer through type I (purple) and type II photoprocesses (yellow).

absorption of these compounds in the therapeutic window (600−1000 nm) and thereby to reach deep-seated solid tumors. Unfortunately, the lowering of tumor pO_2 distant from blood vessels remains an obstacle for the use of classical photosensitizers because of the need of PDT for molecular oxygen to initiate cell death.[8−10] Recent studies have however shown that

type I photoreactivity can lead to strong cytotoxic effects under low oxygen conditions.[11−18] Innovative strategies, involving this pathway, have thus recently been developed to overcome the problem of tumor hypoxia.[8] Nevertheless, it remains an underexplored research area, and hypoxic-active type I photosensitizers are still scarcely reported.

Consequently, we have concentrated our efforts on developing novel molecules able to cause cellular damage by exploiting type I processes. We have opted for bis-cyclometalated Ir(III) complexes because they form lipophilic cations characterized by a rapid cellular uptake[19−21] and tunable redox properties.[22−24] Actually, we have recently reported on novel Ir(III)-based compounds with long-lived triplet excited states[25] and strong photo-oxidizing powers.[26] Our goal is now to examine whether the intracellular oxygen content influences their photocytotoxicity. Viability assays have been performed on 2D cell cultures under both normoxic and hypoxic conditions as well as on 3D tumor spheroids. These models are particularly suited for this study, due to the development of a spontaneous hypoxic core.[27]

■ RESULTS AND DISCUSSION

Two Ir(III) complexes, namely, Ir-pzpy and Ir-TAP (Figure 2), have been synthesized and purified as previously described
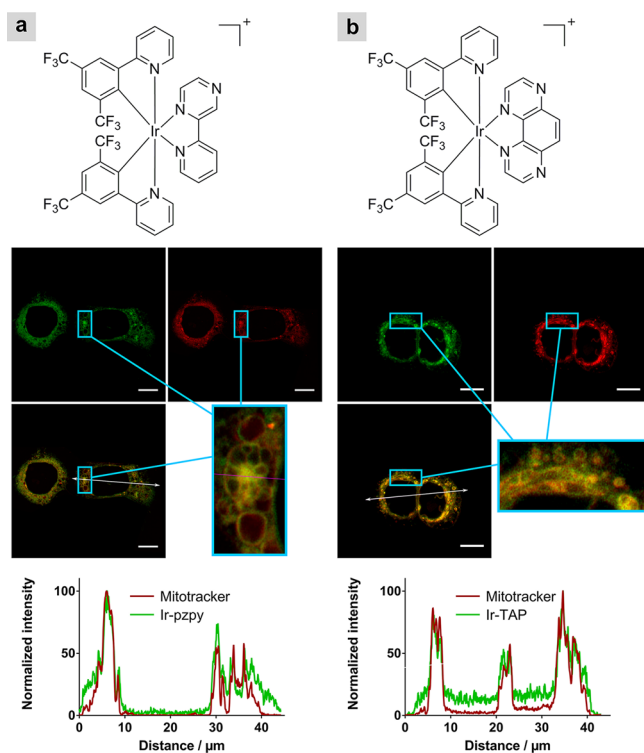

Figure 2. Live confocal imaging of FaDu cancer cells after 1 h of incubation with 20 μM (a) Ir-pzpy and (b) Ir-TAP. The Ir(III) photosensitizers are in green, and the Mitotracker Red CMXROS is in red. A plot profile across the cell (white arrow) is also shown for each photosensitizer. Scale bars: 100 μM.

(Supporting Information).[25,26] Confocal microscopy of FaDu cancer cells (Figure 2) reveals a rapid uptake of both compounds upon 1 h incubation time. Co-localization experiments with subcellular markers show that these drugs are mainly mitochondria-accumulated (Pearson's correlation coefficient of 0.81 and 0.93 for Ir-pzpy and Ir-TAP, respectively), which is

consistent with many other examples of positively charged Ir(III) complexes, reaching these organelles by energy-dependent or -independent pathways.[28−31] Such a subcellular localization may actually constitute a key feature for Ir(III)-based molecules through the induction of mitochondrial dysfunction and associated cell death pathways, as reported for various mitochondria-targeting compounds.[32,33]

The capacity of both Ir(III)-based drugs to initiate cell death has been assessed on FaDu and HT-29 cancer cells, under normoxic (21% O_2) and hypoxic (1% O_2) conditions. The IC_{50} values (Table 1), obtained by plotting viability vs log

Table 1. IC_{50} Values Determined from Dose-Dependent Growth Inhibitory Curves of Ir-pzpy and Ir-TAP on FaDu and HT-29 Cancer Cells, in the Dark and upon Light Activation, under Normoxic (21% O_2) and Hypoxic (1% O_2) Conditions[a]

cell type	Ir-pzpy/μM		Ir-TAP/μM	
	light (dark)	PI[b]	light (dark)	PI[b]
FaDu				
normoxia	3.8 ± 0.4 (69.4 ± 6.2)	18.4	5.4 ± 0.4 (>100)	>18.5
hypoxia	18.1 ± 1.8 (79.6 ± 7.1)	4.4	12.8 ± 0.7 (>100)	>7.8
HT-29				
normoxia	8.7 ± 0.7 (>100)	>11.5	12.0 ± 0.5 (>100)	>8.3
hypoxia	28.6 ± 2.3 (96.2 ± 6.2)	3.4	24.2 ± 1.5 (>100)	>4.3

[a]Cells were treated during 1 h with the desired concentration of complex, before being irradiated or not for 30 min with 405 nm LEDs (light dose = 2.83 J/cm^2). The amount of viable cells was determined 24 h later by WST-1 viability assays. The data obtained in three independent experiments (4 wells/condition) are expressed as mean + standard deviation. [b]PI = photoindex = IC_{50} dark/IC_{50} light.

concentration (Figure S1), show that whereas the dark toxicity of both complexes is relatively low in the studied concentration range, cell viability decreases dramatically upon light excitation (light dose = 2.83 J/cm^2). This light-triggered cytotoxic effect though reduced at lower pO_2 due to the inhibition of type II photoprocesses is still significant for both compounds under hypoxia, which supports possible contribution of oxygen-independent type I processes. Interestingly, lowering pO_2 affects in a different way the photocytotoxicity of both sensitizers, with hypoxia/normoxia IC_{50} ratios amounting to 3.3−4.8 for Ir-pzpy and 2.0−2.4 for Ir-TAP upon light excitation. A possible explanation for this phenomenon arises from the longer excited state lifetime of Ir-pzpy in water ($\tau_{Ir\text{-}pzpy}$ = 297 ns) as compared to Ir-TAP ($\tau_{Ir\text{-}TAP}$ = 56 ns) and thus its stronger sensitivity toward the amount of dissolved oxygen. This result reflects the better capacity of Ir-pzpy to generate $^1O_2$ through a type II photoreaction and is consistent with the $^1O_2$ quantum yields, determined for each complex in water (Φ_Δ Ir-pzpy = 0.68, Φ_Δ Ir-TAP = 0.08) (Figure S2 and Table S1). These data support a model wherein the anticancer activity of Ir-pzpy relies more on a classical type II PDT pathway than the one of Ir-TAP, which exhibits thus a stronger cytotoxic activity in the absence of oxygen.

The above hypothesis has been confirmed by photocleavage experiments carried out on a supercoiled pBR322 plasmid (Figure 3). While both drugs are inactive in the dark, Ir-pzpy shows a strong cleavage activity upon 30 min irradiation with 405 nm LEDs (Figure 3). Indeed, at concentrations exceeding 10 μM, the bands attributed to the supercoiled conformation disappear, whereas open-circular as well as linear plasmid
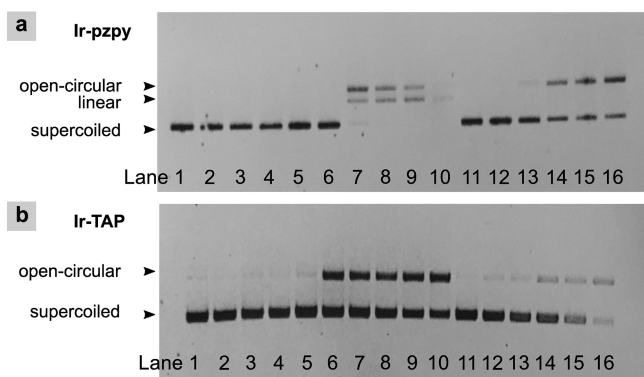
Figure 3. Agarose (0.8%) gel electrophoresis of supercoiled pBR322 plasmid DNA (260 ng) exposed to (a) Ir-pzpy for 30 min and (b) Ir-TAP for 120 min. Lane 1: pBR322 control dark, lane 2: pBR322 control + NaN$_3$ (10 mM) dark, lane 3: pBR322 + Ir (25 μM) dark, lane 4: pBR322 + Ir (25 μM) + NaN$_3$ (10 mM) dark, lanes 5−10: pBR322 + Ir (0, 5, 10, 15, 20, 25 μM) light, lanes 11−16: pBR322 + Ir (0, 5, 10, 15, 20, 25 μM) + NaN$_3$ (10 mM) light.

conformations appear (lanes 5−10) (Figure 3a). However, as expected from the model described above, the addition of a singlet oxygen scavenger (NaN$_3$) decreases dramatically the cleavage activity of Ir-pzpy. Only the open-circular conformation is obtained, and it coexists with the supercoiled form, even at the highest complex concentrations. By contrast, the photocleavage activity of Ir-TAP though reduced due to its shorter excited state lifetime is less affected by the addition of sodium azide. With or without the singlet oxygen scavenger, the supercoiled conformation is always present and only the open-circular form can be obtained (Figure 3b). This result is consistent with its lower ^{1}O$_2$ quantum yield as compared to Ir-pzpy. Finally, it is worth noting that these experiments demonstrate unambiguously that the PDT activity of both complexes not only relies on ^{1}O$_2$ sensitization but also involves type I processes.

In order to explore the cell death mechanism initiated by Ir(III) complexes upon light excitation, flow cytometric analyses of FaDu cancer cells double-labeled with annexin V-FITC and propidium iodide have been performed (Figures S3 and S4). As shown in the Supporting Information, nontreated cells remain viable, with cell mortality inferior to 10%. By contrast, treatments with Ir-pzpy and Ir-TAP induce cytotoxicity, which increases with the drug dose as well as over the time after the irradiation step. For both drugs, at intermediate concentrations, early apoptosis is detected, which suggests that cell mortality mainly occurs by apoptotic pathways.

In addition to the experiments conducted on 2D cancer cell monolayers, the oxygen-dependence of the Ir(III) complexes anticancer activity has also been examined in 3D tumor spheroids. As proven in the Supporting Information (Figure S5), FaDu tumor spheroids are characterized by the development of a spontaneous hypoxic core surrounded by a normoxic continuum, thereby recapitulating the different compartments, with lower or higher oxygen levels, observed in a tumor *in vivo*. Moreover, matrix and cell−cell interactions within these 3D multicellular aggregates make them particularly suited to study drug penetration and, in the specific context of photosensitizers, to evaluate the capacity of light to reach them deep in the tissues.[27,34]

Viability assays performed on 3D tumor spheroids confirm the primary conclusions drawn from the experiments conducted

on 2D cell cultures. Whereas the cytotoxicity of both drugs is weak in the dark (Figure 4a and Figure S7), the light activation
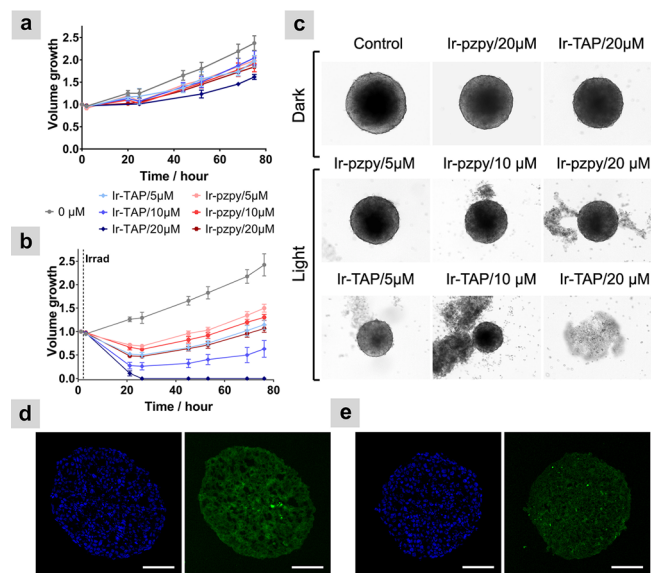

Figure 4. (a) Dark- and (b) light-induced cytotoxic effect of Ir-pzpy and Ir-TAP on tumor spheroids (diameter: 350−400 μm) obtained from 3D cultures of FaDu cancer cells. A time line summarizing this experiment is given in Figure S6. The volume growth of spheroids is plotted as a function of time. At day 5, the spheroids were incubated without drugs or with Ir-pzpy or Ir-TAP for 24 h. They were then exposed (t = 1 h) or not to 405 nm LEDs for 30 min (light dose = 2.83 J/cm^2). (c) Representative pictures of 3D FaDu tumor spheroids 24 h after the irradiation step. (d, e) Representative picture of sections (5 μm) obtained by physical slicing of FaDu tumor spheroids after 24 h of incubation with 20 μM (d) Ir-pzpy and (e) Ir-TAP. The Ir(III)-based photosensitizers are in green, and nuclei stained with DraqS are in blue. Scale bars: 100 μm.

(light dose = 2.83 J/cm^2) induces a dramatic decrease in cancer cell viability (Figure 4b and Figure S8). Importantly, the effects of both complexes are consistent with results obtained with cell monolayers under hypoxia. Indeed, Ir-TAP shows larger growth inhibitory effects toward tumor spheroids than Ir-pzpy, which supports a pronounced activity of the former when hypoxia is present in the system. The cell death associated with the phototoxicity of Ir-pzpy is actually limited to surface cell layers and does not vary a lot with the drug concentration (Figure 4b,c and Figure S8). By contrast, the cytotoxic effects, arising from light-activated Ir-TAP, are detected deep in the 3D cellular aggregates, even in strong hypoxic areas (Figure 4b,c and Figure S8).

A lack of light penetration cannot account for the failure of Ir-pzpy to inhibit the spheroid growth. Indeed, although both complexes possess the same absorption properties on the excitation wavelength ($\varepsilon_{405\ nm}$ = ±800 M^{-1}·cm^{-1} for both compounds) (Figure S11), Ir-TAP (20 μM) can induce the complete destruction of the spheroidal structure and has therefore a stronger photoactivity than Ir-pzpy at the same concentration. In addition, a problem of drug penetration can be excluded because luminescent signals arising from each Ir(III) complex have been observed at different depths in the 3D multicellular aggregates. These luminescent signals are actually homogeneously distributed in the different z-stacks analyzed by confocal microscopy (Figure S12), but also over whole deep-

seated sections obtained by physical slicing of FaDu tumor spheroids (Figure 4d,e).

The incomplete destruction of spheroids by Ir-pzpy is likely to be associated with its stronger sensitivity to oxygen and its subsequent higher dependence on type II processes. In 3D multicellular models, such a phenomenon has already been reported on several well-known PDT sensitizers, including Photofrin, 5-aminolevulinic acid (ALA), and hypericin.[35−38] Actually, whereas the supply of oxygen is limited in tumor spheroids, the photoproduction of $^1O_2$ by these compounds induces a rapid depletion of pO_2 inside the 3D structure. Consequently, the anticancer activity of strong type II sensitizers, such as those mentioned above and Ir-pzpy, decreases dramatically. Usually, a reduction of the light dose leads to the recovery of their antiproliferative effect by diminishing the oxygen consumption rate. Fractional photodynamic therapy may also be considered for these compounds.[39] However, as reported by Evans et al.,[40] the use of type I sensitizers represents another promising approach. Indeed, thanks to their lower oxygen consumption rate and their ability to induce cellular damage at low pO_2, they show a great activity in 3D tumor spheroids. Such a behavior is verified herein with Ir-TAP, which is characterized by a high photo-oxidizing power as well as a low $^1O_2$ quantum yield and which presents an exquisite therapeutic effect in spontaneously hypoxic spheroid models.

In order to increase the growth inhibitory effect of Ir-pzpy, fractional PDT with two irradiation steps (light dose/irradiation = 2.83 J/cm^2) at a 24 h interval has been carried out. As expected, an additional reduction in the spheroid volume has been observed due to tissue reoxygenation (Figure 5a,b and
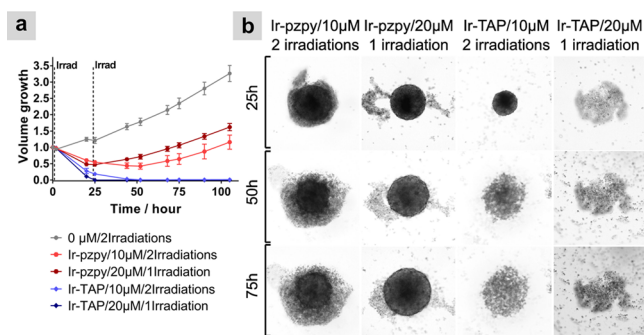

Figure 5. (a) Cytotoxic effect of Ir-pzpy and Ir-TAP on tumor spheroids (diameter: 350−400 μm) obtained from 3D cultures of FaDu cancer cells. A time line summarizing this experiment is given in Figure S9. The volume growth of spheroids is plotted as a function of time. At day 5, spheroids were incubated without drugs or with Ir-pzpy or Ir-TAP for 24 h. They were then exposed once ($t = 1$ h) (light dose = 2.83 J/cm^2) or twice ($t = 1$ and 24 h) (light dose = 5.66 J/cm^2) to 405 nm LEDs for 30 min. (b) Representative pictures of 3D FaDu tumor spheroids at different times.

Figure S10). In addition, it is worth noting that the combination of two separated irradiation steps at a lower drug concentration (10 μM) has been found to be more efficient than a single irradiation step at a higher concentration (20 μM). A similar experiment has also been performed using Ir-TAP as photosensitizer. In this case, fractional PDT has allowed us to decrease the drug concentration used from 20 μM to 10 μM, while keeping an important cytotoxic effect and inducing the complete destruction of the 3D multicellular aggregates (Figure 5a,b and Figure S10).

CONCLUSION

In conclusion, we showed that photo-oxidizing iridium(III) complexes represent an attractive family of photosensitizers to treat tumors. Indeed, as reported for other Ir(III)-based compounds, they are characterized by a rapid cellular uptake and the capacity to penetrate deep into 3D tumor spheroids.[41−43] In addition, thanks to their subcellular localization, they are able to induce rapid apoptotic cell death upon light excitation. Between the two Ir(III)-based drugs studied here, Ir-TAP has emerged as the most promising candidate by combining a low $^1O_2$ quantum yield and the capacity to initiate type I oxygen-independent processes. A complete destruction of 3D tumor spheroids has been observed at a concentration of 20 μM, but also at 10 μM in combination with two irradiation steps at a 24 h interval. By contrast, the therapeutic activity of the second compound, Ir-pzpy, remains limited in such models. Actually, this phenomenon has been attributed to its rapid consumption of all the oxygen available in the spheroid, as previously proven for other strong $^1O_2$ sensitizers. However, thanks to fractional PDT, an increased growth inhibitory effect could be obtained with Ir-pzpy.

These results open the door to future studies investigating the anticancer effect of both drugs *in vivo*. Nevertheless, in this context, the short activation wavelength (405 nm) of our drugs might be an issue when it comes to light penetration in living tissues. Consequently, the use of two-photon excitation will also be examined. Indeed, several recent studies have shown that photocytotoxic Ir(III) complexes could be excited through the absorption of two low-energy photons instead of one high-energy photon.[44−50]

ASSOCIATED CONTENT

Ⓢ Supporting Information

The Supporting Information is available free of charge on the ACS Publications website at DOI: 10.1021/jacs.9b07723.

> Experimental and synthetic details, 2D cell viability curves, representative pictures of 3D tumor spheroids, $^1O_2$ quantum yield data, UV−visible spectra of Ir-pzpy and Ir-TAP, and additional confocal imaging (PDF)

AUTHOR INFORMATION

Corresponding Authors
*olivier.feron@uclouvain.be
*benjamin.elias@uclouvain.be

ORCID Ⓘ
Robin Bevernaegie: 0000-0003-1605-9253

Present Address
§Department of Microbiology and Molecular Medicine, University Medical Centre (C.M.U.), Rue Michel-Servet 1, 1211 Geneva 4, Switzerland.

Notes
The authors declare no competing financial interest.

■ REFERENCES

(1) Wilson, B. C; Patterson, M. S The physics, biophysics and technology of photodynamic therapy. *Phys. Med. Biol.* 2008, 53, R61.

(2) Agostinis, P.; Berg, K.; Cengel, K. A.; Foster, T. H.; Girotti, A. W.; Gollnick, S. O.; Hahn, S. M.; Hamblin, M. R.; Juzeniene, A.; Kessel, D.; Korbelik, M.; Moan, J.; Mroz, P.; Nowis, D.; Piette, J.; Wilson, B. C.; Golab, J. Photodynamic therapy of cancer: An update. *Ca-Cancer J. Clin.* 2011, 61, 250−281.

(3) Bown, S. G. Photodynamic therapy for photochemists. *Philos. Trans. R. Soc., A* 2013, 371, 371.

(4) Mroz, P.; Yaroslavsky, A.; Kharkwal, G. B.; Hamblin, M. R. Cell Death Pathways in Photodynamic Therapy of Cancer. *Cancers* 2011, 3, 2516.

(5) Castano, A. P.; Mroz, P.; Hamblin, M. R. Photodynamic therapy and anti-tumour immunity. *Nat. Rev. Cancer* 2006, 6, 535.

(6) Ormond, A.; Freeman, H. Dye Sensitizers for Photodynamic Therapy. *Materials* 2013, 6, 817.

(7) Monro, S.; Colon, K. L.; Yin, H.; Roque, J., 3rd; Konda, P.; Gujar, S.; Thummel, R. P.; Lilge, L.; Cameron, C. G.; McFarland, S. A. Transition Metal Complexes and Photodynamic Therapy from a Tumor-Centered Approach: Challenges, Opportunities, and Highlights from the Development of TLD1433. *Chem. Rev.* 2019, 119, 797−828.

(8) Li, X.; Kwon, N.; Guo, T.; Liu, Z.; Yoon, J. Innovative Strategies for Hypoxic-Tumor Photodynamic Therapy. *Angew. Chem., Int. Ed.* 2018, 57, 11522−11531.

(9) Wilson, W. R.; Hay, M. P. Targeting hypoxia in cancer therapy. *Nat. Rev. Cancer* 2011, 11, 393.

(10) Pinto, A.; Mace, Y.; Drouet, F.; Bony, E.; Boidot, R.; Draoui, N.; Lobysheva, I.; Corbet, C.; Polet, F.; Martherus, R.; Deraedt, Q.; Rodríguez, J.; Lamy, C.; Schicke, O.; Delvaux, D.; Louis, C.; Kiss, R.; Kriegsheim, A. V.; Dessy, C.; Elias, B.; Quetin-Leclercq, J.; Riant, O.; Feron, O. A new ER-specific photosensitizer unravels 1O2-driven protein oxidation and inhibition of deubiquitinases as a generic mechanism for cancer PDT. *Oncogene* 2016, 35, 3976.

(11) Lv, Z.; Wei, H.; Li, Q.; Su, X.; Liu, S.; Zhang, K. Y.; Lv, W.; Zhao, Q.; Li, X.; Huang, W. Achieving efficient photodynamic therapy under both normoxia and hypoxia using cyclometalated Ru(ii) photosensitizer through type I photochemical process. *Chem. Sci.* 2018, 9, 502−512.

(12) Ding, H.; Yu, H.; Dong, Y.; Tian, R.; Huang, G.; Boothman, D. A.; Sumer, B. D.; Gao, J. Photoactivation switch from type II to type I reactions by electron-rich micelles for improved photodynamic therapy of cancer cells under hypoxia. *J. Controlled Release* 2011, 156, 276−280.

(13) Gilson, R. C.; Black, K. C. L.; Lane, D. D.; Achilefu, S. Hybrid TiO2−Ruthenium Nano-photosensitizer Synergistically Produces Reactive Oxygen Species in both Hypoxic and Normoxic Conditions. *Angew. Chem., Int. Ed.* 2017, 56, 10717−10720.

(14) Arenas, Y.; Monro, S.; Shi, G.; Mandel, A.; McFarland, S.; Lilge, L. Photodynamic inactivation of Staphylococcus aureus and methicillin-resistant Staphylococcus aureus with Ru(II)-based type I/ type II photosensitizers. *Photodiagn. Photodyn. Ther.* 2013, 10, 615−625.

(15) Lameijer, L. N.; Ernst, D.; Hopkins, S. L.; Meijer, M. S.; Askes, S. H. C.; Le Dévédec, S. E.; Bonnet, S. A Red-Light-Activated Ruthenium-Caged NAMPT Inhibitor Remains Phototoxic in Hypoxic Cancer Cells. *Angew. Chem., Int. Ed.* 2017, 56, 11549−11553.

(16) Novohradsky, V.; Rovira, A.; Hally, C.; Galindo, A.; Vigueras, G.; Gandioso, A.; Svitelova, M.; Bresolí-Obach, R.; Kostrhunova, H.; Markova, L.; Kasparkova, J.; Nonell, S.; Ruiz, J.; Brabec, V.; Marchán, V. Towards Novel Photodynamic Anticancer Agents Generating Superoxide Anion Radicals: A Cyclometalated IrIII Complex Conjugated to a Far-Red Emitting Coumarin. *Angew. Chem., Int. Ed.* 2019, 58, 6311−6315.

(17) Novohradsky, V.; Vigueras, G.; Pracharova, J.; Cutillas, N.; Janiak, C.; Kostrhunova, H.; Brabec, V.; Ruiz, J.; Kasparkova, J. Molecular superoxide radical photogeneration in cancer cells by dipyridophenazine iridium(iii) complexes. *Inorg. Chem. Front.* 2019, 6, 2500−2513.

(18) He, L.; Zhang, M.-F.; Pan, Z.-Y.; Wang, K.-N.; Zhao, Z.-J.; Li, Y.; Mao, Z.-W. A mitochondria-targeted iridium(iii)-based photoacid generator induces dual-mode photodynamic damage within cancer cells. *Chem. Commun.* 2019, 55, 10472−10475.

(19) Caporale, C.; Massi, M. Cyclometalated iridium(III) complexes for life science. *Coord. Chem. Rev.* 2018, 363, 71−91.

(20) McKenzie, L. K.; Bryant, H. E.; Weinstein, J. A. Transition metal complexes as photosensitisers in one- and two-photon photodynamic therapy. *Coord. Chem. Rev.* 2019, 379, 2−29.

(21) Zamora, A.; Vigueras, G.; Rodríguez, V.; Santana, M. D.; Ruiz, J. Cyclometalated iridium(III) luminescent complexes in therapy and phototherapy. *Coord. Chem. Rev.* 2018, 360, 34−76.

(22) Deaton, J. C.; Castellano, F. N. In *Iridium(III) in Optoelectronic and Photonics Applications*; Zysman-Colman, E., Ed.; John Wiley & Sons Ltd., 2017; pp 1−69.

(23) Weynand, J.; Bonnet, H.; Loiseau, F.; Ravanat, J. L.; Dejeu, J.; Defrancq, E.; Elias, B. Targeting G-Rich DNA Structures with Photoreactive Bis-Cyclometallated Iridium(III) Complexes. *Chem. - Eur. J.* 2019, 25, 12730−12739.

(24) Lentz, C.; Schott, O.; Auvray, T.; Hanan, G.; Elias, B. Photocatalytic Hydrogen Production Using a Red-Absorbing Ir(III)-Co(III) Dyad. *Inorg. Chem.* 2017, 56, 10875−10881.

(25) Bevernaegie, R.; Marcelis, L.; Moreno-Betancourt, A.; Laramee-Milette, B.; Hanan, G. S.; Loiseau, F.; Sliwa, M.; Elias, B. Ultrafast charge transfer excited state dynamics in trifluoromethyl-substituted iridium(iii) complexes. *Phys. Chem. Chem. Phys.* 2018, 20, 27256−27260.

(26) Bevernaegie, R.; Marcélis, L.; Laramée-Milette, B.; De Winter, J.; Robeyns, K.; Gerbaux, P.; Hanan, G. S.; Elias, B. Trifluoromethyl-Substituted Iridium(III) Complexes: From Photophysics to Photo-oxidation of a Biological Target. *Inorg. Chem.* 2018, 57, 1356−1367.

(27) Kimlin, L. C.; Casagrande, G.; Virador, V. M. In vitro three-dimensional (3D) models in cancer research: An update. *Mol. Carcinog.* 2013, 52, 167−182.

(28) Wang, B.; Liang, Y.; Dong, H.; Tan, T.; Zhan, B.; Cheng, J.; Lo, K. K.-W.; Lam, Y. W.; Cheng, S. H. A Luminescent Cyclometalated Iridium(III) Complex Accumulates in Mitochondria and Induces Mitochondrial Shortening by Conjugation to Specific Protein Targets. *ChemBioChem* 2012, 13, 2729−2737.

(29) Cao, J. J.; Tan, C. P.; Chen, M. H.; Wu, N.; Yao, D. Y.; Liu, X. G.; Ji, L. N.; Mao, Z. W. Targeting cancer cell metabolism with mitochondria-immobilized phosphorescent cyclometalated iridium(iii) complexes. *Chem. Sci.* 2017, 8, 631−640.

(30) Ouyang, M.; Zeng, L.; Huang, H.; Jin, C.; Liu, J.; Chen, Y.; Ji, L.; Chao, H. Fluorinated cyclometalated iridium(iii) complexes as mitochondria-targeted theranostic anticancer agents. *Dalton Trans* 2017, 46, 6734−6744.

(31) Lo, K. K.-W.; Chan, B. T.-N.; Liu, H.-W.; Zhang, K. Y.; Li, S. P.-Y.; Tang, T. S.-M. Cyclometalated iridium(iii) polypyridine dibenzo-cyclooctyne complexes as the first phosphorescent bioorthogonal probes. *Chem. Commun.* 2013, 49, 4271−4273.

(32) Chakrabortty, S.; Agrawalla, B. K.; Stumper, A.; Vegi, N. M.; Fischer, S.; Reichardt, C.; Kögler, M.; Dietzek, B.; Feuring-Buske, M.; Buske, C.; Rau, S.; Weil, T. Mitochondria Targeted Protein-Ruthenium Photosensitizer for Efficient Photodynamic Applications. *J. Am. Chem. Soc.* 2017, 139, 2512−2519.

(33) Battogtokh, G.; Ko, Y. T. Mitochondrial-targeted photosensitizer-loaded folate-albumin nanoparticle for photodynamic therapy of cancer. *Nanomedicine* 2017, 13, 733−743.

(34) Doix, B.; Bastien, E.; Rambaud, A.; Pinto, A.; Louis, C.; Grégoire, V.; Riant, O.; Feron, O. Preclinical Evaluation of White Led-Activated

Non-porphyrinic Photosensitizer OR141 in 3D Tumor Spheroids and Mouse Skin Lesions. *Front. Oncol.* **2018**, *8*, 8.

(35) Hilf, R.; Gibson, S. L.; Foster, T. H. *Mechanisms contributing to optimization of PDT with first-generation photosensitizers*; SPIE, 1993; Vol. *1881*.

(36) Madsen, S. J.; Sun, C.-H.; Tromberg, B. J.; Wallace, V. P.; Hirschberg, H. Photodynamic Therapy of Human Glioma Spheroids Using 5-Aminolevulinic Acid. *Photochem. Photobiol.* **2000**, *72*, 128−134.

(37) Kamuhabwa, A. A.; Huygens, A.; De Witte, P. A. Photodynamic therapy of transitional cell carcinoma multicellular tumor spheroids with hypericin. *Int. J. Oncol.* **2003**, *23*, 1445−50.

(38) Kamuhabwa, A. R.; Huygens, A.; Roskams, T.; De Witte, P. A. Enhancing the photodynamic effect of hypericin in human bladder transitional cell carcinoma spheroids by the use of the oxygen carrier, perfluorodecalin. *Int. J. Oncol.* **2006**, *28*, 775−80.

(39) Weston, M. A.; Patterson, M. S. Validation and Application of a Model of Oxygen Consumption and Diffusion During Photodynamic Therapy In Vitro. *Photochem. Photobiol.* **2014**, *90*, 1359−1367.

(40) Evans, C. L.; Abu-Yousif, A. O.; Park, Y. J.; Klein, O. J.; Celli, J. P.; Rizvi, I.; Zheng, X.; Hasan, T. Killing Hypoxic Cell Populations in a 3D Tumor Model with EtNBS-PDT. *PLoS One* **2011**, *6*, No. e23434.

(41) Sun, L.; Li, G.; Chen, X.; Chen, Y.; Jin, C.; Ji, L.; Chao, H. Azo-Based Iridium(III) Complexes as Multicolor Phosphorescent Probes to Detect Hypoxia in 3D Multicellular Tumor Spheroids. *Sci. Rep.* **2015**, *5*, 14837.

(42) Sun, L.; Chen, Y.; Kuang, S.; Li, G.; Guan, R.; Liu, J.; Ji, L.; Chao, H. Iridium(III) Anthraquinone Complexes as Two-Photon Phosphorescence Probes for Mitochondria Imaging and Tracking under Hypoxia. *Chem. - Eur. J.* **2016**, *22*, 8955−8965.

(43) Zhang, P.; Huang, H.; Banerjee, S.; Clarkson, G. J.; Ge, C.; Imberti, C.; Sadler, P. J. Nucleus-Targeted Organoiridium-Albumin Conjugate for Photodynamic Cancer Therapy. *Angew. Chem., Int. Ed.* **2019**, *58*, 2350−2354.

(44) Zhou, Z.; Liu, J.; Rees, T. W.; Wang, H.; Li, X.; Chao, H.; Stang, P. J. Heterometallic Ru−Pt metallacycle for two-photon photodynamic therapy. *Proc. Natl. Acad. Sci. U. S. A.* **2018**, *115*, 5664−5669.

(45) Starkey, J. R.; Pascucci, E. M.; Drobizhev, M. A.; Elliott, A.; Rebane, A. K. Vascular targeting to the SST2 receptor improves the therapeutic response to near-IR two-photon activated PDT for deep-tissue cancer treatment. *Biochim. Biophys. Acta, Gen. Subj.* **2013**, *1830*, 4594−4603.

(46) Starkey, J. R.; Rebane, A. K.; Drobizhev, M. A.; Meng, F.; Gong, A.; Elliott, A.; McInnerney, K.; Spangler, C. W. New Two-Photon Activated Photodynamic Therapy Sensitizers Induce Xenograft Tumor Regressions after Near-IR Laser Treatment through the Body of the Host Mouse. *Clin. Cancer Res.* **2008**, *14*, 6564−6573.

(47) Samkoe, K. S.; Clancy, A. A.; Karotki, A.; Wilson, B. C.; Cramb, D. T. Complete blood vessel occlusion in the chick chorioallantoic membrane using two-photon excitation photodynamic therapy: implications for treatment of wet age-related macular degeneration. *J. Biomed. Opt.* **2007**, *12*, 1−14.

(48) McKenzie, L. K.; Sazanovich, I. V.; Baggaley, E.; Bonneau, M.; Guerchais, V.; Williams, J. A. G.; Weinstein, J. A.; Bryant, H. E. Metal Complexes for Two-Photon Photodynamic Therapy: A Cyclometallated Iridium Complex Induces Two-Photon Photosensitization of Cancer Cells under Near-IR Light. *Chem. - Eur. J.* **2017**, *23*, 234−238.

(49) Qiu, K.; Ouyang, M.; Liu, Y.; Huang, H.; Liu, C.; Chen, Y.; Ji, L.; Chao, H. Two-photon photodynamic ablation of tumor cells by mitochondria-targeted iridium(iii) complexes in aggregate states. *J. Mater. Chem. B* **2017**, *5*, 5488−5498.

(50) Liu, J.; Jin, C.; Yuan, B.; Liu, X.; Chen, Y.; Ji, L.; Chao, H. Selectively lighting up two-photon photodynamic activity in mitochondria with AIE-active iridium(iii) complexes. *Chem. Commun.* **2017**, *53*, 2052−2055.